Ballistic electron transmission in coupled parallel waveguides

Y. Takagaki and K. Ploog
Paul-Drude-Institut für Festkörperelektronik, Hausvogteiplatz 5-7, 10117 Berlin, Germany
(Received 7 September 1993)

Four-terminal resistances in parallel electron-waveguide structures coupled by a window region are calculated using classical- and quantum-mechanical methods. An electron incident through one of the waveguides can travel into the other in the quantum ballistic regime. The transmission coefficients into the ends of the second waveguide oscillate as one of the sample parameters, such as the separation between the waveguides or the Fermi energy, is varied, leading to quasiregular modulations in the transfer resistance. Several different mechanisms are responsible for the oscillations including (i) classical specular reflections from the side wall of the window region, (ii) depopulation of quasi-one-dimensional subbands in the waveguides, and (iii) Fabry-Perot-type quantum interference in the window region. We propose that these scenarios of the oscillations can be distinguished experimentally by their peculiar dependence on the system parameters.

I. INTRODUCTION

The electron transport in microstructures created in high mobility GaAs-$Al_xGa_{1-x}As$ heterostructures bears a strong resemblance to the propagation of electromagnetic waves in waveguides.[1] In samples having dimensions of less than the elastic mean free path l_e, due to the remote impurities and residual impurities in the channels, the Drude theory is no longer applicable since impurity scattering does not play a role. The conductance of the system is solely influenced by the geometrical features. When the phase-coherence length of an electron exceeds the sample size at low temperatures, the Fermi wavelength λ_F provides another important length scale since the conductance is modified due to quantum interference effects as the sample dimensions vary on the order of λ_F.[1] The problem can be viewed as a quantum scattering problem,[2] and hence it is required to solve the Schrödinger equation in determining the scattering coefficients between one-dimensional (1D) transmission channels. Electron devices utilizing the fully quantum-mechanical nature of the transport have been proposed based on their analogy with microwave and optical devices.[3–5]

A considerable number of anomalous ballistic effects have been observed in the resistance measured in cross junctions of quasi-1D wires, including the quenched[6] or negative[7] Hall resistance and the negative bend resistance.[8] Surprisingly, these features can be reproduced by the classical billiard model, in which the transmission coefficients are examined by simply following ballistic trajectories in the sample geometries.[9] If the corners of the cross region are rounded, which is the case in the experimental situation due to screening, many electrons are reflected from the diagonal wall into the wrong Hall probe, or electrons multiply reflected in the expanded intersection region have equal opportunity to exit on either side at very weak magnetic fields.[7,9] This rebound and scrambling trajectories are responsible for the anomalous phenomena in the Hall resistance.[10]

Recently, Hirayama *et al.*[11] have investigated the transport properties in parallel wires directly coupled by a ballistic window. The coupling in this geometry takes place in a direction perpendicular to the electron propagation in the infinite wires, so that the transmission reflects the angular distribution of the incident electrons. The transfer resistance, which we define in Sec. II, becomes negative when the sample size is reduced to below l_e, in contrast to a positive value in a diffusive transport sample. It was observed in this ballistic regime that an oscillation was superimposed on the resistance as the width of the channel was varied.[11] The experiment was performed at relatively high temperatures so that the quantum interference effect was expected to be less important. The oscillation was thus interpreted in terms of the depopulation of 1D subbands in the terminal wires. Interestingly, in the smallest sample, in which the clearest oscillation was observed as expected, the resistance oscillated between negative and positive values.[11]

It is the purpose of this paper to present numerical results for the resistances in the parallel wire structures. Although the interpretation of the oscillation in terms of the subband effect will be confirmed to be reasonable, we propose an alternative mechanism which may account for the oscillation. This explanation is based on the classical rebound effect in a straight wire, and it may be tested by measuring the temperature dependence of the oscillation. We will also show that quantum-mechanical interference leads to oscillations in the resistance if the system is entirely phase coherent.

II. NUMERICAL MODEL

We model the geometry as illustrated in Fig. 1. Two parallel infinite waveguides of width W are connected by a transverse waveguide with width D and length L. We set $D=W$ throughout the paper unless otherwise noted. We take an electrostatic potential which is zero within the channels, and infinite outside. The Coulomb interac-

tions between electrons are ignored so that the Coulomb blockade is assumed not to play a role in our results.[12] The transport in the structure is treated as a scattering problem of a noninteracting electron system in the linear-response regime. Generally, the individual transmission coefficients among the leads are not accessible in the experiments, though it is possible to measure them as demonstrated in a recent experiment.[13] For convenience, to compare with the experimental results, we define four-terminal resistances in the structure, i.e., the longitudinal resistance $R_L = R_{13,24}$, the transfer resistance $R_T = R_{12,34}$, and the generalized Hall resistance $R_H = R_{23,14}$, where $R_{ij,kl} = (V_k - V_l)/I_{i-j}$ indicates that the voltage difference is measured between leads k and l while the current flows from lead i to lead j. These resistances are related to the transmission coefficients of an electron at the Fermi energy $E_F = \hbar^2 k_F^2/2m$ through the Büttiker-Landauer formula.[2] Because of the symmetry of the structure, the transmission in the absence of a magnetic field is described by the four transmission probabilities indicated in Fig. 1, which we denote T, S_F, S_B, and R. We thus have

$$R_L = \frac{h}{2e^2} \frac{T - S_F}{(S_B + T)(S_B + S_F)} , \tag{1a}$$

$$R_H = \frac{h}{2e^2} \frac{T - S_B}{(S_F + T)(S_F + S_B)} , \tag{1b}$$

$$R_T = \frac{h}{2e^2} \frac{S_B - S_F}{(T + S_B)(T + S_F)} . \tag{1c}$$

It is easy to show that[14]

$$R_T = R_L - R_H . \tag{2}$$

We note that, in the current and voltage probe configurations for R_T, the voltage probes are separated from the nominal current path, and hence R_T is useful to characterize any nonlocal behavior of the transport.[15] The local resistances R_L and R_H, on the other hand, contain the conventional "bulk" resistance if the impurity scattering is not completely negligible. In the classical diffusive transport limit, it is expected that $R_L = R_H$, and $R_T = 0$, since $S_F = S_B$.

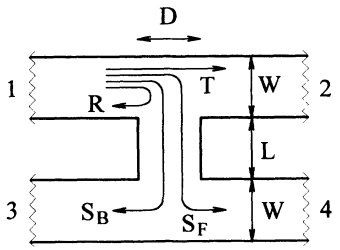

FIG. 1. Schematic view of the coupled parallel waveguides. Four reservoirs attached to the semi-infinite leads are labeled 1–4. The four-terminal resistances of the system are determined by the transmission probabilities T, S_F, S_B, and R, in the absence of magnetic field. We assume $D = W$ except in Figs. 3 and 6.

III. CLASSICAL TRANSMISSION

We first describe the classical mechanism of the oscillation. Hirayama *et al.*[11] observed an oscillation in R_T, which is proportional to the difference between the transmission probabilities into each side of the second waveguide, $S_B - S_F$. Obviously, $S_F > S_B$, as L is short since the direct transmission from lead 1 to lead 4 is significant. However, this diagonal trajectory is shadowed by the sidewall of the window region when L is increased. The rebound trajectory reflected from the facing wall into lead 3, illustrated by the dotted line in the middle inset of Fig. 2(a), will eventually become dominant, leading to $S_F < S_B$ which results in an inversion of the polarity of R_T.[7] When L is further increased, the electron is reflected twice in the window region (the right inset), and R_T will again become negative. Therefore, R_T will exhibit an oscillation according to the number of reflections from the walls in the window region.

In order to confirm the above idea, we have numerically calculated the transmission coefficients employing classical and quantum-mechanical methods. In Figs. 2 and 3, we show the transmission and the resistances evaluated by the billiard model.[9] The transmission probabilities are determined by counting the number of classical trajectories which reach each terminal lead as electrons are injected from one of the leads with uniform distribution over the channel width W and $\cos\theta$ dependence on the incident angle θ.[9,16] The reflections from the waveguide walls are assumed to be specular.[17] Because electrons prefer to move straight instead of turning around the

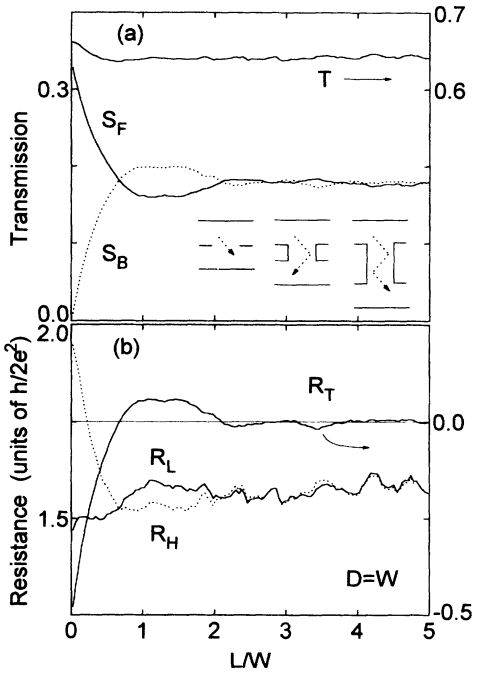

FIG. 2. (a) Transmission probabilities and (b) resistances calculated by the billiard model as a function of the separation L between two parallel wires of width W. In the classical case, $R = 0$. The transmission becomes independent of L for larger separation. The inset illustrates the direct (left), rebound (center), and multiply reflected (right) trajectories which lead to an oscillation in R_T for smaller L.

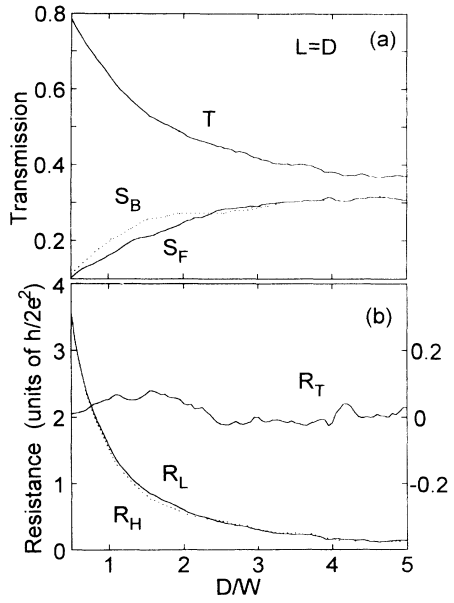

FIG. 3. (a) Classical transmission probabilities and (b) resistances as a function of D/W when the aspect ratio of the window region is fixed at $L/D=1$.

corner and, obviously, $S_B \to 0$ for $L \to 0$, R_T is negative for $L \sim 0$.[8,11] The dependence of the resistances on L shown in Fig. 2(b) indicates that R_T indeed exhibits an oscillatory behavior and ranges between negative and positive values due to the classical mechanism mentioned above. When for $L > 3W$ the electrons are reflected many times from the walls, S_F and S_B become comparable and nearly independent on L because of the broad angular distribution of injection, resulting in the rapid decay of the oscillation. Notice that R_L and R_H are almost identical in this multiple reflection regime, whereas they deviate from each other as the oscillatory behavior in R_T is evident for smaller L. The straight-through transmission is almost independent of L for $L > 0.5W$ since the electrons hardly see the second waveguide directly.[18] The decrease of T compared to the $L=0$ case makes R_L roughly independent of L.

In the experiments of Hirayama *et al.*, the in-plane gate voltage applied to the terminal wires mainly modifies the width of the parallel wires, while the size of the window region is almost unchanged.[19] Figure 3 gives results corresponding to this situation. The transmission straight through the initial waveguide approaches unity as the entrance of the window region is narrowed because of the fixed total transmission. Since $L=D$, S_B is expected to be larger than S_F due to the rebound effect. This tendency is clear for smaller D/W.[20] When the width of the waveguides is reduced relative to the window region, all the transmission probabilities (except for $R=0$) become comparable since the angular distribution of the flux injected into the window region becomes broad. An oscillation may be present in R_T. However, its amplitude is comparable with the statistical error.

We have emphasized that the broad distribution of the flux in the window region is detrimental to the oscillation. Although the oscillation is found to be weak, it may be enhanced in the experimental situation due to the forward collimation of the injected electron beam.[21] The distribution of electrons departed from a gradually widened channel is sharpened in the forward direction.[16,22] If the channel width varies adiabatically from W to W_m, the angular distribution is restricted within a cone of an angle $\theta_{\max}=\sin^{-1}(W/W_m)$.[22] An improved oscillation may appear particularly in the magnetic-field dependence rather than in the L dependence. Beenakker and van Houten[9] have discussed oscillatory behaviors of R_T as a function of magnetic field due to electron focusing in narrow wires. Our results indicate that an oscillation due to a similar mechanism can take place even in the absence of magnetic field. Although the mechanism of the transmission modulation is classical, the magnetoresistance oscillation is sensitive to temperature since thermal smearing of the Fermi distribution, which is equivalent to a nonuniform cyclotron radius $\hbar k_F/eB$, corresponds to a magnetic-field averaging.[9] It is essentially impossible to distinguish the oscillation from the phenomena of quantum-mechanical origin in terms of the temperature dependence. The oscillation we have discussed, on the other hand, is insensitive to temperatures since the thermal velocity distribution does not affect the results. For simplicity, we have neglected the rounded geometry of the corners in our model. In the presence of the rounding, S_F and S_B depend chaotically on magnetic fields due to the scrambling effect in the intersection region, leading to irregular fluctuations in R_T.[9,15] It is thus important to take into account the rounded geometry when one calculates the magnetic-field dependence of the transmission.[23] However, the chaotic scrambling effect is not important in the zero-magnetic-field case.[24]

IV. QUANTUM-MECHANICAL TRANSMISSION

We now turn to a discussion of quantum-mechanical results. The phase-coherence length is a length scale over which the phase information of an electron is retained and thus quantum-mechanical interference takes place. At finite temperatures, quantum interference effects deteriorate because of phase breaking due to inelastic scattering. We thus assume zero temperature, and that all scattering effects are neglected. The transmission probabilities were then determined by means of the waveguide-matching method.[25] Details of the transmission properties depend strongly on the system parameters, and especially λ_F, which does not appear in the classical simulation, is now an important length scale. In general, the clearest quantum-mechanical effects are expected in the single-mode regime, and the transmission approaches classical behavior as the number of occupied modes $N=[k_F W/\pi]$ is increased.

A. Depopulation of transverse modes

In Fig. 4, we show transmission probabilities as a function of wave vector for three different window lengths (a) $L=0$, (b) $L=0.5D$, and (c) $L=D$. The classical values indicated by the thin lines are in good agreement with the

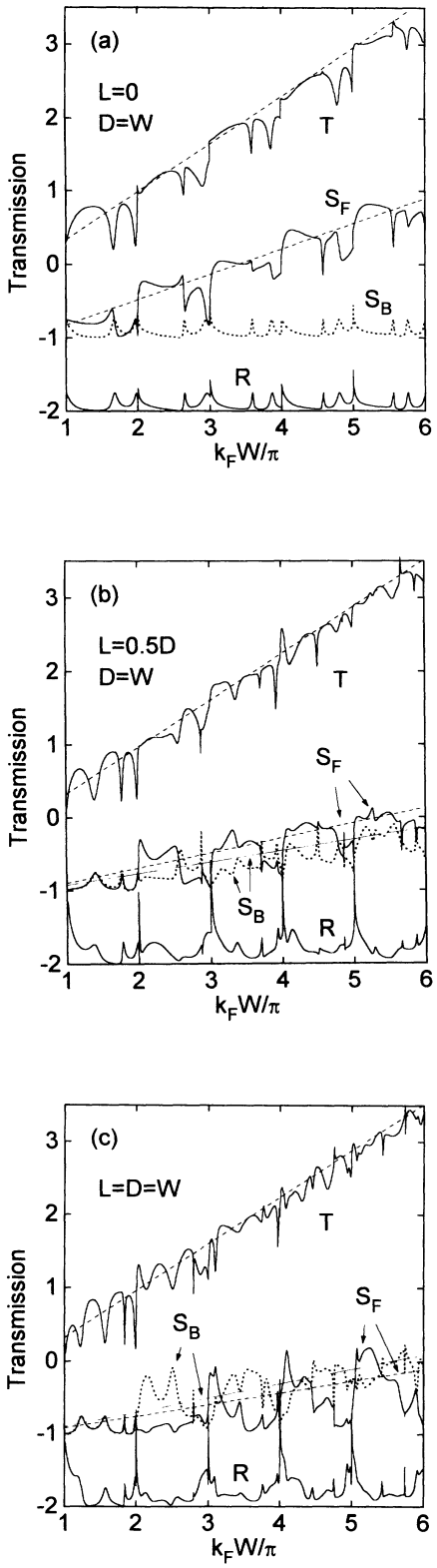

FIG. 4. Quantum-mechanical transmission probabilities as a function of $k_F W/\pi$ for $L=$(a) 0, (b) $0.5D$, and (c) D. The thin lines represent the corresponding classical values, for which the total flux is reduced by $\frac{1}{2}$. In the classical limit, these three cases correspond to (a) $S_F > S_B = 0$, (b) $S_F > S_B > 0$, and (c) $S_B > S_F$ due to the rebound effect. The curves for S_F, S_B, and R are offset by -1, -1, and -2, respectively.

average behavior of the quantum-mechanical results.[26] Here the amount of the incident flux $k_F W/\pi$ is reduced by $\frac{1}{2}$, which corresponds to the suppression due to the quantum zero-point motion in the transverse direction. The correction to the total classical flux is also adopted in the following when compared with the quantum-mechanical results. In the classical case $R=0$, and hence R remains small as the injected flux is increased. It is the same with S_B for $L=0$, as shown in Fig. 4(a). Near the subband thresholds, substantial deviations from classical values appear as dips in T and peaks in R, since additional scattering channels become available. When the energy is barely above the thresholds, the trapping times of the electron in the scattering region are very long, and hence the electron suffers significant backscattering. The singularities are enhanced as L is increased. The momentum of electrons with energy slightly above the threshold is considerably transverse directed, and hence the transmission probabilities turning around the corner into the second waveguide are large. The electron is more forward directed as the energy is increased for a fixed mode number.[27] This trend is evident for $L=0$, where T increases whereas the transmission into the second waveguide decreases until a higher-lying mode falls below E_F. It is interesting that this ballistic nature is, in a sense, reversed when S_F and S_B are concerned. We would expect naively that the diagonal transmission S_F is preferable to S_B, at least when $L=0$, as the electron is forward directed. However, S_F exhibits maxima when the energy is slightly above the threshold, and decreases with increasing energy irrespective of L/D. The average behavior of S_B, on the other hand, is roughly independent of energy. Note that S_B exceeds S_F when the electrons are forward directed for $L=D$. A natural explanation for this phenomenon is that the rebound trajectory makes a major contribution to the transmission, and the electron is scattered from the sidewall of the window region into the opposite lead.

In order to examine these characteristics in more detail, in Fig. 5 we show the transmission probabilities as a function of the incident mode for different wave vectors and L/D ratios. The lower-lying modes tend to go straight since the momentum is forward directed, while S_F becomes larger when the momentum is transverse directed for the higher-lying modes. Therefore, major contributions to S_B generally come from midlying modes. This provides the reason the quantum-mechanical transmission exhibits somewhat unusual dependencies on system parameters. For $L=D$, S_F is larger than S_B when the energy is slightly above the propagation thresholds, and it becomes smaller than S_B when the energy is slightly below the thresholds. We also see this trend in individual modes. On the other hand, S_B is always larger than S_F for the lower-lying modes when $L=0.5D$. Because the higher-lying modes strongly tend to go to lead 4 rather than to lead 3, S_F summed over the modes becomes larger than S_B.

In addition to the subband effect, resonant structures due to quasibound states in the window region emerge in Fig. 4, and the number of the transmission resonances in-

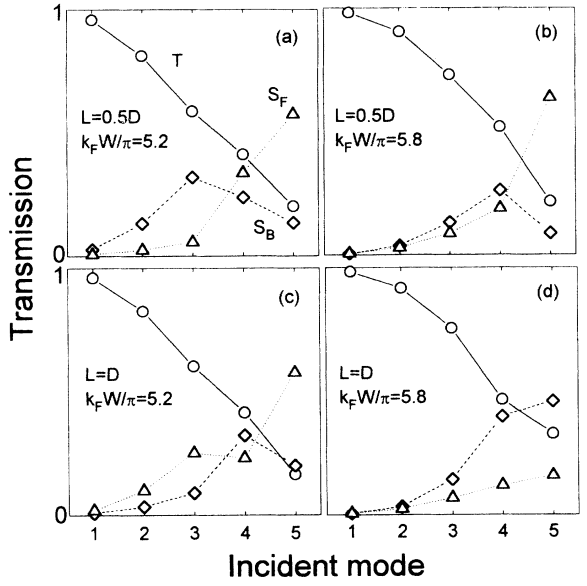

FIG. 5. Transmission probabilities T (solid line), S_F (dotted line), and S_B (dashed line), when the electron is injected through individual modes are plotted. The transmission summed over the injected modes into each side of the second waveguide show $S_F > S_B$ for (a), (b), and (c), whereas $S_F < S_B$ for (d).

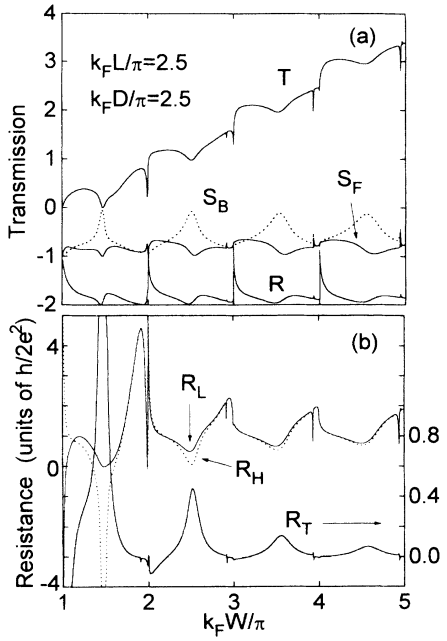

FIG. 6. Dependence of (a) quantum transmission and (b) resistances on the width of the parallel waveguides. The dimensions of the window region are fixed at $k_FL/\pi = k_FD/\pi = 2.5$. (a) The curves for S_F, S_B, and R are offset by -1, -1, and -2, respectively.

creases as L gets longer.[4,28,29] Coherent multiple reflections of the electron from the sample boundaries occur at the resonances, and so the electron is transmitted equally from the quasibound states to all the leads since the waveguide widths are equivalent, leading to $T \approx S_F \approx S_B \approx R \approx \frac{1}{4}$ in the single-mode regime. This resembles the classical scrambling effect.[9] The unusual relations between the transmission probabilities are particularly remarkable. When $L=0$, S_B and R are surprisingly almost identical over the entire energy range, whereas S_B coincides with S_F for $L=0.5D$ and D in the single-mode regime.

The oscillatory behavior in the previous case arises from the population of modes in both the terminal waveguides and the window region. In Fig. 6, W is varied relative to λ_F while $L=D$ is fixed at $k_FL/\pi=2.5$ to highlight the role of the mode population in the terminal waveguides. The results are compared with the corresponding classical case shown in Fig. 3. When increasing the number of propagating modes ($D/W \to 0$), T increases while S_F, S_B, and R remain small in agreement with the classical behavior. The electron is again strongly reflected from the junction just above the mode thresholds in the terminal waveguides. Since $L=D$, transmission S_B is enhanced, whereas S_F is suppressed with increasing energy for a fixed mode number similar to Fig. 4(c). Figure 6(b) shows that the modulation in the transmission leads to oscillations in the resistances. Notice that, unlike R_L and R_H, the singularities in T and R at the mode thresholds do not necessarily result in an oscillation in R_T. The rebound effect, i.e., the length of the window region, has important influences on the details of the oscillation in R_T, as indicated in Fig. 4. The amplitude of the oscillation in $S_B - S_F$ only slightly decreases as W is increased, and so the amplitude in R_T is inversely proportional to N. The oscillation due to the classical pinball in this situation is indicated to be weak in Fig. 3, so that the oscillatory behavior is ascribed to the quantum-mechanical subband effect. Near $k_FW/\pi = 1.47$, R_T and R_H reveal a divergence, since S_B becomes nearly unity and the other three transmission probabilities are almost zero.

B. Fabry-Perot-type interference

Quantum interference in the scattering from the two T-shaped junctions gives rise to oscillations in the transmission as the distance between the parallel waveguides is varied analogously to the optical Fabry-Perot device. The clearest oscillation is expected in the single-mode regime. In Fig. 7(a), the transmission probabilities are plotted as a function of the separation between the waveguides for $k_FW/\pi=1.5$. The average values of the transmission probabilities do not depend on L/W and agree with the classical predictions in the long-L limit, indicated by the dashed arrows. The peaks in S_F, S_B, and R occur in phase while they coincide with the dips in the transmission straight through the incident waveguide since the total transmission is fixed. At these "resonance" conditions of L/W, the transmissions into the four leads are nearly identical. As expected, the period agrees with one-half of the longitudinal wavelength $\lambda_\parallel$ in the window region. Notice that S_B possesses interesting relations to the other transmission probabilities. Until S_B reaches the first peak when L is increased ($L < 0.3W$), it

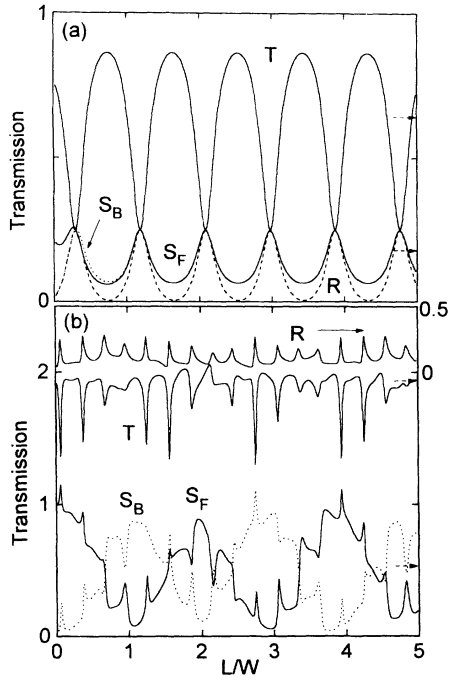

FIG. 7. Quantum transmission probabilities are plotted as a function of the length of the window region for $k_F W/\pi$=(a) 1.5 and (b) 3.5. (a) As L/W is increased, $S_B \simeq R$ until S_B reaches the first peak, whereas $S_B \simeq S_F$ after the second peak. The classical values of the transmission probabilities are indicated by the dashed arrows. The width of the window region is assumed to be $D = W$.

is nearly identical with R and then becomes identical with S_F for $L > W$, as indicated in Fig. 4.

The transmission is more complicated in the multiple-mode case, since each mode has different $\lambda_\parallel$. We show the transmission probabilities when three modes are occupied ($k_F W/\pi = 3.5$) in Fig. 7(b). The average values of the transmission probabilities again agree with the classical values. We find a short-period small-amplitude modulation in all four transmission probabilities, and a long-period large-amplitude modulation in the transmissions passing through the window region. The amplitude of the rapid oscillation shows a beat structure due to mixing of different fundamental frequencies. The Fabry-Perot resonances in the rapid modulation always appear as narrow peaks in R and dips in T, whereas they can be either peaks or dips in S_F and S_B. Nevertheless, these structures occur nearly simultaneously, and the period roughly corresponds to the $\lambda_\parallel$ of the lower-lying mode. The slowly varying large-amplitude oscillations in S_F and S_B are out of phase, and lead to an oscillation in R_T as will be shown below. The rapid modulation, on the other hand, does not have a definite phase relation. The period of the slow modulation is much larger than the $\lambda_\parallel$ of any three modes and agrees with the mixing frequency due to the lowest and second modes. Baranger[20] has investigated the oscillations in double-junction waveguide structures, in which two semi-infinite waveguides are attached to an infinite waveguide at right angles. It is found that the period of the rapid oscillation corresponds, in contrast to our case, to the $\lambda_\parallel$ of the higher-lying mode. This may be ascribed to the fact that the direction of the electron incidence is parallel to the Fabry-Perot interferometer in Baranger's case, while it is transverse in our case. When the electron is injected through the main waveguide, the interferometer is fairly transparent for the lower-lying modes, and the multiple reflection between the junctions is significant for the higher-lying modes.

The resistances obtained from the transmission probabilities in Fig. 7 are shown in Fig. 8. Note that the situation corresponds to the classical case shown in Fig. 2. In the single-mode case, the L dependence of R_T is similar to the classical one, though the position of the peak does not agree with the classical result, evidencing that the modulation is related to the rebound mechanism. In the region where the modulation in R_T disappears, R_L and R_H are identical as they are in the classical case. However, R_L and R_H exhibit an oscillation produced by the Fabry-Perot interference in contrast to the classical case. Remarkably, this Fabry-Perot interference is not reflected in R_T. The oscillation in R_T in the multiple-mode case, on the other hand, does not attenuate as L is increased. It is thus apparent that this oscillation arises from a different scenario, though part of the oscillation for smaller L may be related to the classical rebound mechanism. Since the large-period oscillation in S_F and S_B is out of phase, it does not show up in R_L and R_H, as

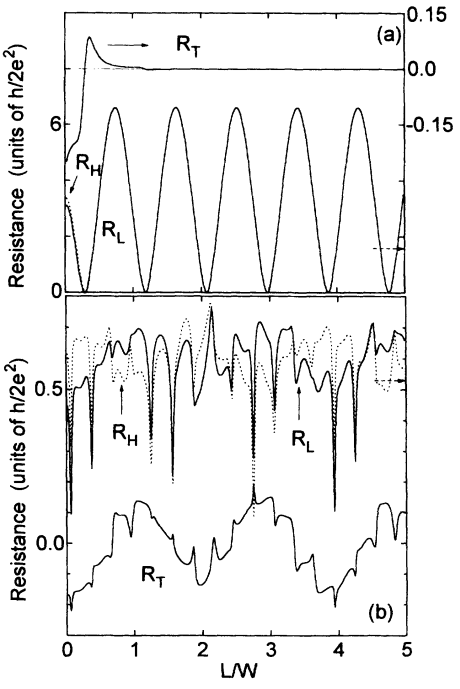

FIG. 8. Transfer resistance, longitudinal resistance, and Hall resistance (dotted line) calculated from the transmission probabilities in Fig. 7 as a function of the separation between the waveguides. The Fermi energy is taken to be $k_F W/\pi$=(a) 1.5 and (b) 3.5. (a) For larger L/W, R_L and R_H overlap with each other. The classical values of the resistances are indicated by the dashed arrows.

can be derived from Eqs. (1a) and (1b). It is surprising that it is the single-mode case which shows a resemblance to the classical case instead of the multiple-mode case. Because of the quantum-mechanical mixing of modes, R_L and R_H do not coincide in the multiple-mode case. The average values of R_L and R_H, however, do not vary with length, and correspond approximately to the classical prediction.

V. SUMMARY

We have investigated possible mechanisms for the oscillatory behavior of the transfer resistance measured in coupled parallel wires in the ballistic regime. The subband depopulation in the terminal wire is found to produce an oscillation in the transfer resistance. We point out that it is not the enhanced backscattering at the subband thresholds but the incident-angle-dependent reflection in the window region which causes the oscillation. We find that the classical rebound trajectory gives rise to an oscillation when the length of the window region is small. This mechanism could be dominant if $k_B T$ is larger than the subband spacing. At lower temperatures, oscillations can occur due to Fabry-Perot-type quantum interference in the window region, provided that the whole system is phase coherent. The period of the oscillation is large and determined by the mixing of various modes in the wire.

ACKNOWLEDGMENT

We thank G. Junk for reading the manuscript.

[1]For a review, see C. W. J. Beenakker and H. van Houten, in *Solid State Physics,* edited by H. Ehrenreich and D. Turnbull (Academic, New York, 1991), Vol. 44, p. 1.

[2]M. Büttiker, Phys. Rev. Lett. **57**, 1761 (1986).

[3]S. Datta, M. R. Melloch, S. Bandyopadhyay, R. Noren, M. Vaziri, M. Miller, and R. Reifenberger, Phys. Rev. Lett. **55**, 2344 (1985).

[4]F. Sols, M. Macucci, U. Ravaioli, and K. Hess, Appl. Phys. Lett. **54**, 350 (1989); J. Appl. Phys. **66**, 3892 (1989).

[5]J. A. del Alamo and C. C. Eugster, Appl. Phys. Lett. **56**, 78 (1990); N. Tsukada, A. D. Wieck, and K. Ploog, *ibid.* **56**, 2527 (1990).

[6]M. L. Roukes, A. Scherer, S. J. Allen, Jr., H. G. Craighead, R. M. Ruthen, E. D. Beebe, and J. P. Harbison, Phys. Rev. Lett. **59**, 3011 (1987).

[7]C. J. B. Ford, S. Washburn, M. Büttiker, C. M. Knoedler, and J. M. Hong, Phys. Rev. Lett. **62**, 2724 (1989).

[8]Y. Takagaki, K. Gamo, S. Namba, S. Ishida, S. Takaoka, K. Murase, K. Ishibashi, and Y. Aoyagi, Solid State Commun. **68**, 1051 (1988).

[9]C. W. J. Beenakker and H. van Houten, Phys. Rev. Lett. **63**, 1857 (1989); and in *Electronic Properties of Multilayers and Low-Dimensional Semiconductor Structures,* edited by J. M. Chamberlain, L. Eaves, and J. C. Portal (Plenum, New York, 1990).

[10]T. Geisel, R. Ketzmerick, and O. Schedletzky, Phys. Rev. Lett. **69**, 1680 (1992).

[11]Y. Hirayama, A. D. Wieck, T. Bever, K. von Klitzing, and K. Ploog, Phys. Rev. B **46**, 4035 (1992).

[12]C. W. J. Beenakker, H. van Houten, and A. A. Staring, in *Granular Nanoelectronics,* edited by D. K. Ferry, J. R. Barker, and C. Jacoboni (Plenum, New York, 1991), p. 359.

[13]K. L. Shepard, M. L. Roukes, and B. P. van der Gaag, Phys. Rev. B **46**, 9648 (1992).

[14]This relation is not satisfied if the symmetry of the transmission is not exact.

[15]Y. Takagaki, K. Gamo, S. Namba, S. Takaoka, and K. Murase, Solid State Commun. **75**, 873 (1990).

[16]H. U. Baranger, D. P. DiVincenzo, R. A. Jalabert, and A. D. Stone, Phys. Rev. B **44**, 10 637 (1991).

[17]T. J. Thornton, M. L. Roukes, A. Scherer, and B. P. Van der Gaag, Phys. Rev. Lett. **63**, 2128 (1989).

[18]The straight-through transmission into lead 2 without passing the window region is $(\sqrt{5}-1)/2=0.618$, and so about 4% (7%) of T in the limit $L\rightarrow\infty(0)$ is due to reflections from the second waveguide.

[19]M. Yamada, K. Hirakawa, T. Odagiri, T. J. Thornton, and T. Ikoma, Superlatt. Microstruct. **11**, 261 (1992).

[20]H. U. Baranger, Phys. Rev. B **42**, 11 479 (1990).

[21]H. U. Baranger and A. D. Stone, Phys. Rev. Lett. **63**, 414 (1989).

[22]C. W. J. Beenakker and H. van Houten, Phys. Rev. B **39**, 10 445 (1989).

[23]R. A. Jalabert, H. U. Baranger, and A. D. Stone, Phys. Rev. Lett. **65**, 2442 (1990).

[24]M. L. Roukes and O. L. Alerhand, Phys. Rev. Lett. **65**, 1651 (1990).

[25]Y. Takagaki and D. K. Ferry, Phys. Rev. B **45**, 12 152 (1992).

[26]The total transmission in the classical simulation is unity while it is the number of propagating modes N in the quantum-mechanical simulation. The resistances for the quantum-mechanical case are hence scaled by a factor N compared to the classical results.

[27]Y. Avishai and Y. B. Band, Phys. Rev. Lett. **62**, 2527 (1989); G. Kirczenow, Solid State Commun. **71**, 469 (1989).

[28]R. L. Schult, D. G. Ravenhall, and H. W. Wyld, Phys. Rev. B **39**, 5476 (1989).